Universiteit Leiden
The Netherlands

Arabidopsis AGC3 kinases and PIN plasma membrane abundance

Gelderen, K. van

Citation

Gelderen, K. van. (2017, July 6). *Arabidopsis AGC3 kinases and PIN plasma membrane abundance*. Retrieved from https://hdl.handle.net/1887/50504

Version:	Not Applicable (or Unknown)
License:	Licence agreement concerning inclusion of doctoral thesis in the Institutional Repository of the University of Leiden
Downloaded from:	https://hdl.handle.net/1887/50504

Note: To cite this publication please use the final published version (if applicable).

Cover Page

Universiteit Leiden

Leiden University Repository

The handle http://hdl.handle.net/1887/50504 holds various files of this Leiden University dissertation

Author: Gelderen, Kasper van
Title: Arabidopsis AGC3 kinases and PIN plasma membrane abundance
Issue Date: 2017-07-06

Chapter 4

An INDEHISCENT-controlled auxin response specifies the separation layer in early *Arabidopsis* fruit

Kasper van Gelderen[1,2]*, Martin van Rongen[1,3]*, An'an Liu[1], Anne Otten[1], Remko Offringa[1,#]

Published in Molecular Plant, June 6 2016. Volume 9, issue 6, page 857-69.
doi: 10.1016/j.molp.2016.03.005.

[1] Plant developmental genetics, Institute of Biology, Leiden University, Sylviusweg 72, 2333 BE Leiden, The Netherlands.
[2] Current affiliation: Plant Ecophysiology, Institute of Environmental Biology, Utrecht University, 3584 CH Utrecht, The Netherlands.
[3] Current affiliation: Sainsbury Laboratory, 47 Bateman Street, Cambridge CB2 1LR, United Kingdom.
[#] Author for correspondence: r.offringa@biology.leidenuniv.nl

* These authors contributed equally

Abstract

Seed dispersal is an important moment in the life cycle of a plant species, since it optimises chances for survival. *Arabidopsis* seeds are dispersed through the dehiscence of fruit containing the seed – a tightly regulated process. The transcription factor INDEHISCENT (IND) mediates dehiscence by specifying the valve margin tissue that forms at the border between the valves (carpel walls) and the central replum. The valve margin is composed of a layer of lignified cells and a narrow separation layer that upon fruit ripening separate the valve and replum by secreting cell wall-degrading enzymes. IND has been proposed to specify the separation layer by inducing a local auxin minimum at late stages of fruit development. However, *IND* is also strongly expressed in the valve margin at early stages of development. Here we describe morphological differences between *ind* mutant and wild-type fruit arising prior to the formation of the separation layer. Our results show that reduced abundance of the PIN FORMED3 (PIN3) auxin efflux carrier coincides with an increased auxin response in the valve margin during early fruit development and that the concomitant onset of cell divisions that form the dehiscence zone is lacking in the *ind* mutant fruit. Furthermore, we show that *IND* promoter-driven expression of the AGC kinases PINOID (PID) and WAG2 induces indehiscence presumably by expelling auxin from the valve margin at stage 13 and 14 of fruit development through increased abundance of the PIN3 auxin efflux carrier. Our results refine the existing model by showing that IND is required at early stages of *Arabidopsis* fruit development to facilitate the auxin-triggered cell divisions that form the dehiscence zone through repression of PID and WAG2 kinase expression.

Introduction

A correct timing of fruit and seed ripening and the subsequent dispersal of the seeds is important to ensure the survival of the next plant generation. This also requires proper patterning of the gynoecium from which the fruit develops. The *Arabidopsis* gynoecium - and that of other Brassicaceae - consists of two fused carpels that form the valves. The valves are fused by a valve margin and replum, which is connected internally to the septum and ovules. The valve margins delimit the borders between valves and replum and consist of a separation layer and a layer of lignified cells (Ferrándiz, 2002). At the final stage of fruit development, cells within the separation layer secrete cell wall-degrading enzymes that promote cell separation and the rigidity of the lignified layer aids the separation of the valves from the replum. This process is referred to as dehiscence and results in seed dispersal (For a review, see: Østergaard, 2009). The valve margin is specified by expression of the valve margin identity genes *INDEHISCENT (IND)*, *SHATTERPROOF (SHP1/2)* and *ALCATRAZ* (*ALC),* which is limited to a narrow region on the valve/replum border due to the repressing effect of FRUITFULL (FUL) in the valves and REPLUMLESS (RPL) in the replum (Ferrándiz et al., 2000; Roeder et al., 2003). Subsequent differentiation of the dehiscence zone into a separation- and a lignified layer is determined by SHP1/2 and IND, whereas separation layer specification also requires ALC (Ferrándiz et al., 2000; Girin et al., 2011; Liljegren et al., 2004; Rajani and Sundaresan, 2001).

Previously, it has been reported that the basic helix-loop-helix transcription factor IND is responsible for the formation of an auxin minimum in the dehiscence zone of the fruit at stage 17B and that this auxin minimum is required for separation layer specification (Sorefan et al., 2009). Members of the PIN-FORMED (PIN) family of auxin efflux carriers have been proposed to play an important role in the establishment of this auxin minimum, as overexpression of IND in seedlings was found to lead to PIN1 and PIN3 polarity loss. IND and the bHLH transcription factor SPATULA (SPT) were found to bind the promoters of the AGC kinase genes *PINOID* (*PID*) and *WAG2* and to repress *PID* and upregulate *WAG2* expression in seedlings (Girin et al., 2011; Sorefan et al., 2009). Since the PID and WAG2 protein kinases are well-established determinants in the subcellular distribution of PIN proteins (Benjamins et al., 2001; Dhonukshe et al., 2010; Friml et al., 2004; Michniewicz et al., 2007), a model was proposed in which IND/SPT-mediated downregulation of PID prevents shootward relocalization of PIN3, whereas enhanced WAG2 expression promotes lateralization of PIN3, which is necessary to obtain the auxin minimum in the dehiscence zone. This model suggested that PID and WAG2 kinases act antagonistically on PIN3 polarity (Sorefan et al., 2009). However, in other publications PID, WAG1 and WAG2 were shown to act redundantly to promote apical PIN1 localization in the embryo protoderm, shootward PIN2 localization in the root tip (Dhonukshe et al., 2010), or PIN3 outer lateral abundance in hypocotyl endodermis cells (Ding et al., 2011).

In order to further investigate the possible antagonistic role of the PID and WAG2 kinases in dehiscence zone specification, we assessed valve margin specification and fruit opening in plants with altered kinase activity. First, since there is differing data on when dehiscence zone differentiation is initiated (Sorefan et al., 2009; Wu et al., 2006) and since a detailed overview of its development is lacking, we traced valve margin and dehiscence zone development in wild-type fruit from before pollination up until fruit maturation. We compared this development with the *ind-2* mutant, which does not form a valve margin (Liljegren et al., 2004). We then closely investigated the role of auxin and its transport in the process of dehiscence zone differentiation, by visualising auxin distribution and PIN3 localisation at the valve margin in both wild-type and *ind-2* mutant background. Our results indicate that dehiscence zone formation takes place at stages 14 to 16 of fruit development and that this coincides with a reduction in PIN3 abundance and an increase in auxin levels in valve margin cells. Valve margin specific expression of *PID* and *WAG2* resulted in indehiscence, which indicates that the reduced PIN3 abundance requires these redundantly acting AGC kinases to be repressed during dehiscence zone formation.

Results

Dehiscence zone formation is initiated following pollination

The stages of gynoecium and fruit development important for dehiscence zone development are depicted in Fig. 1A and B. *IND* is expressed throughout gynoecium and fruit development including during the formation of an auxin minimum that develops immediately prior to fruit opening (Girin et al., 2011; Sorefan et al., 2009; Wu et al., 2006). Based on previous analysis the formation of the dehiscence zone was suggested to occur through cell division events at stage 15 (Wu et al., 2006) (stages defined in Smyth *et al.*, 1990). Since a detailed anatomical analysis of dehiscence zone formation has not been reported, we followed wild-type and *ind-2* fruit development from stages 11 to 17B through transverse sections of the centre of the fruit. Up until the point of pollination at stage 13 an outline of the valve-replum border is becoming evident, possibly due to growth of neighbouring tissue. However our results did not reveal any obvious cell differentiation occurring in the valve margin up until the point of pollination at stage 13 (Fig. 1C, S1A-C and S2A-C). Just after pollination, at stage 14, cell expansion of the epidermal valve cells and endocarp occurred and sutures started to form between the replum and valves (Fig. 1D and L). Cell divisions that formed the smaller cells of the dehiscence zone started at stage 14 and continued into stage 15 and 16 (Fig. 2F,G and N). These cells continued to differentiate, forming the dehiscence zone at stage 17A and B (Fig. 2I,J and P). At these stages, the dehiscence zone could be identified based on the topology of the small separation layer cells and the more strongly stained lignified layer valve cells (Fig. 1B,I

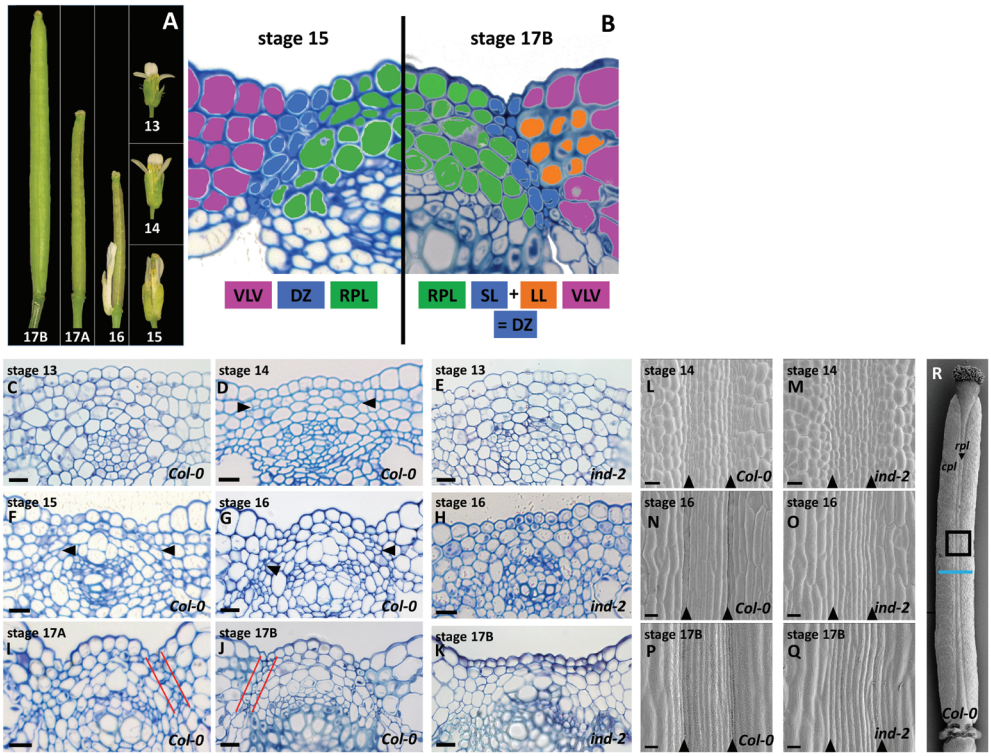

Figure 1: The formation of the dehiscence zone begins at stage 14 of fruit development.

(A) Arabidopsis flowers at stage 13 through 17B of fruit development (Ferrándiz *et al.*, 1999). At stage 13 the anthers extend to the stigmatic tissue and pollination takes place, while fertilization occurs at stage 14. The gynoecium starts to elongate and loses its floral parts from stage 15 to 17B after which the fruit ripens. (B) Coloured transverse sections of stage 15 and 17B fruit showing the valve (VLV, pink), replum (RPL, green) and the dehiscence zone (DZ, blue). At stage 17B the DZ consists of the separation layer (SL, blue) and the lignified layer (LL, orange). (C-K) Transverse sections of toluidine blue-stained *A. thaliana* fruit showing the replum and the valve margins. The blue bar in (R) indicates the approximate location of the sections in the fruit. (C,E) Stage 13 *Col-0* (C) versus *ind-2* (E) gynoecium. (D,F-H) In Stage 14-16 col-0 fruit (D,F,G), divisions (black arrowheads) create the smaller cells that form the dehiscence zone. These divisions or smaller cells are not visible in stage *ind-2* fruit (H). (I-K) In stage 17A and 17B fruit the dehiscence zone (area between red lines) is clearly visible and the toluidine blue staining reveals the slight lignification of the lignified layer. (L-R) Scanning electron microscopy images of stage 14,16, or 17B *Col-0* (L,N,P, R) or *ind-2* (M, O, Q) fruit. The position of the region shown in (L-Q) is indicated by the black box on the stage 17B fruit in (R). The position of the valve margins, characterized by sutures in *Col-0*, are indicated by black arrows.

and J) (Ferrándiz et al., 1999). An earlier report suggested that the cell layers that are formed from stages 14 to 16 are the result of unequal (asymmetric) cell divisions (Wu et al., 2006), which would be in line with the notion that asymmetric cell divisions are formative and generate patterns (De Smet and Beeckman, 2011; Yoshida et al., 2014). Transverse sections indeed suggested that cell divisions in the valve margin might be unequal (Fig.

S1D-F). However, this may be an artefact of the shape of these cells, since they taper at the end (Fig. S1J), and therefore we were unable to unequivocally confirm the asymmetry of these divisions. Nonetheless, our results clearly indicated that dehiscence zone cell differentiation occurs early during fruit development, after fertilization at stages 14 to 16. In line with this observation, no discernible differences in cell topology at the valve margin between wild-type and *ind-2* fruits could be observed prior to fertilization (Fig. 1C and E, S1A-C and S2A-C). However, the cell division and differentiation events occurring in this region after fertilization at stages 14 to 16 in wild-type fruit were completely absent in the *ind-2* mutant (Fig. 1H and K, S1D-F and S2D-F). Our observations are in line with previous analyses (Wu et al., 2006), and show that dehiscence zone formation occurs as early as stage 14 of fruit development, directly after pollination (stage 13) by cell divisions between the valves and replum, producing one or two cell layers that continue to differentiate into the separation layer.

Auxin levels correlate with PIN3 expression during dehiscence zone formation.

Our and previous data suggest that the dehiscence zone forms at stages 14-16 and therefore before the establishment of an auxin minimum at stage 17B. To investigate further the role of auxin during dehiscence zone formation, we traced auxin distribution from stages 11 to 17B in both wild-type and *ind-2* fruits, by correlating the auxin response reporters *DR5::RFP* (Benková et al., 2003) and *35S::DII-YFP* (Brunoud et al., 2012) with the plasma membrane localisation of the predominant PIN in this region, PIN3 (Sorefan et al., 2009). The *35S::DII-YFP* reporter showed that at stage 13, during pollination, auxin was low in the valve, valve margin and replum (Fig. 2A). At stage 14 there was a marked decrease in DII-YFP signal, coinciding with the increase in auxin levels in the fruit (Sorefan et al., 2009), especially in the valve and replum, but surprisingly also in the valve margin (Fig. 2B). At stages 15 and 16 auxin response levels decreased, to increase again at stage 17A, most noticeably in the valve margin (Fig. 2C-E). The auxin-insensitive *35S::mDII-YFP* reporter was used as a control to show that the *35S* promoter is active in all relevant tissues (Fig. 2G and H). The *DR5::RFP* reporter showed a more or less complementary pattern (Fig. 3A-D, I and J) compared to the *35S::DII-YFP* reporter. Although the clear DII-YFP-reported auxin response in the valve margin at stage 14, could not be visualized with *DR5::RFP*, we observed a gradual build-up of auxin response from stages 15 to 17A, and a clear auxin minimum (Sorefan et al., 2009) in the separation layer in stage 17B fruit (Fig. 2F and 3J). Recently it has been shown that the *DR5* reporter in its original guise is a lower affinity binding site for AUXIN RESPONSE FACTORS than previously observed (Boer et al., 2014; Liao et al., 2015), which might explain the differences between *DR5:GFP/RFP* and DII-YFP and also the patchy signal of *DR5::GFP* observed here and elsewhere (Sorefan et al., 2009).

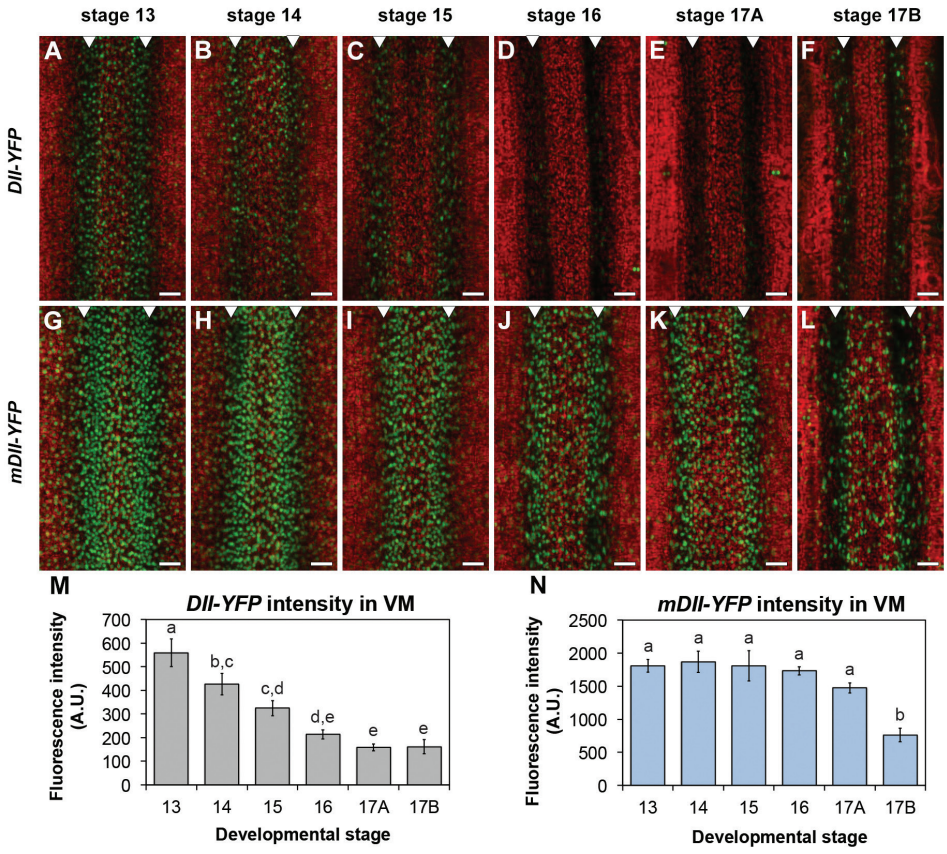

Figure 2: *DII-YFP*-reported auxin response in the valve margin and replum of stage 14 fruit.
Confocal microscopy images of a *35S::DII:YFP-NLS* (*DII-YFP*) *Col-0* stage 13 gynoecium (A), or *35S::DII:YFP-NLS* (*DII-YFP*) *Col-0* stage 14 (B), 15 (C), 16 (D), 17A (E) or 17B (F) fruit, showing the valves, valve margin (white arrows) and replum (scale bar 25 µm). The inset in (F) shows an enlargement of the separation layer. *mDII-YFP* fruits show constitutive YFP signal throughout all tissues during stage 15 and 17A (G and H).

In developing *ind-2* mutant fruit the picture was much simpler. From stage 13 to stage 17A the auxin response around the valve margins was low, and only at stage 17B a sudden increase in auxin response was observed in the replum (Fig. 3O-Q). These results are largely in agreement with previous observations using the *DR5::GFP* reporter (Sorefan et al., 2009), except that our more detailed study detected a significant auxin response in the valve margins of stage 14, 16 and 17A fruits.

Next we correlated PIN3 expression with the auxin response data. In stage 11 and 12 wild-type fruits, PIN3-GFP was weakly visible within the replum and its abundance in this tissue became more clear at stage 13 (Fig. S3A-C), when PIN3-GFP extended to the valve margin (Fig. 3A). PIN3-GFP abundance continued to increase in the valve margin of wild-type fruit at stage 14 and 15, when the first cells of the dehiscence zone could

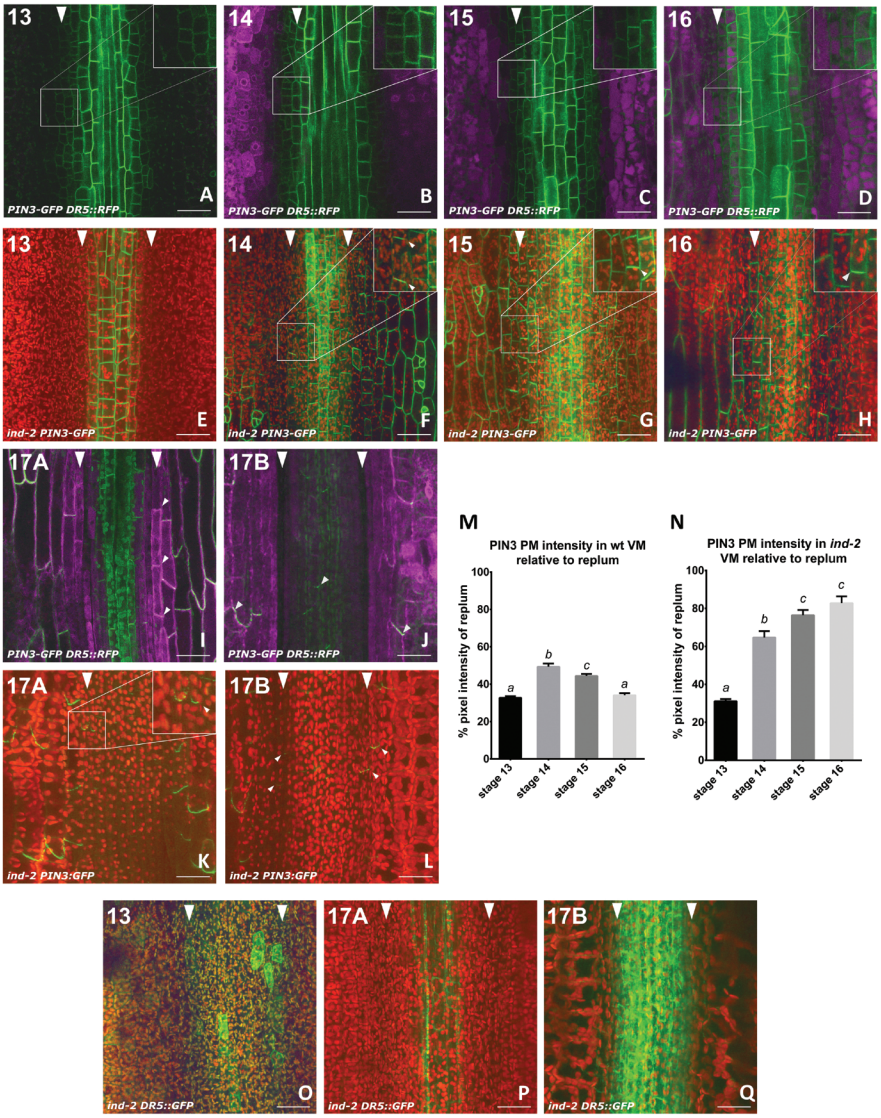

Figure 3: A transiently enhanced auxin response and PIN3-GFP plasma membrane abundance coincide with the establishment of the separation layer in valve margins of early *Arabidopsis* fruit.

(A-L) Combined Z-stack images of tangential confocal sections through the epidermal layer of *pin3 PIN3::PIN3-GFP DR5::RFP* (A-D, I, J), or *ind-2 pin3 PIN3::PIN3-GFP* (E-H, K, L) fruit at stages 13 (A, E), 14 (B, F), 15 (C, G), 16 (D, H), 17A (I, K), and 17B (J, L). Images show PIN3:GFP (green) and RFP (magenta) expression or autofluorescence (red in E-H, K, L) in valves (outer tissues), valve margins (white arrow heads) and replum (inner tissue). The insets in (A-D, F-H, K) show an enlargement of part of the valve margin. (M,N) Quantification of PIN3-GFP plasma membrane signal in the valve margin cells of wild-type fruits. Values relative to replum (M) and absolute values (N) are shown (error bars show SEM, *a, b and c* indicate significant differences between average values in the *t*-test, p<0,05., per stage at least 8 cells per sample and at least 6 biological samples were measured). (O-Q) Combined Z-stack images of tangential confocal sections through the epidermal layer of *ind-2 DR5::GFP* fruit. Images show GFP (green) and autofluorescence (red) in valves (outer tissues), valve margins (white arrow heads) and replum (inner tissue). The scale bar indicates 25 µm.

be identified, while the abundance in the replum remained markedly higher (Fig. 3B-C and S4E). A quantification of the PIN3 plasma membrane signal confirmed that PIN3 in the valve margin increased at stages 14 and 15, and that the increase was strongest at stage 14, when compared with the PIN3 plasma membrane intensity in the replum, while absolute PIN3-GFP levels were highest at stage 15 (Fig. 3M and N). At stage 16 PIN3-GFP started to decrease in the dehiscence zone (Fig. 3D, M and N). This decrease continued prior to maturation at stage 17A, resulting in a weak PIN3-GFP signal in the rootward polar domain (Fig. 3I), which was still visible at stage 17B (Fig. 3J). At stage 17A and 17B the overall PIN3-GFP abundance appeared reduced. PIN3-GFP was clearly expressed in the epidermis of the valves (Fig. S3D-F), but due to the focal plane this was not always visible, when focussing on the expression in the dehiscence zone.

PIN3-GFP localization and abundance in the *ind-2* mutant appeared similar to wild type up until stage 13 (Fig. 3E and S4C). At stage 14 PIN3-GFP abundance in *ind-2* sharply increased throughout the valve, valve margin and replum and this persisted until stage 16 (Fig. 3E-H and S4G-I), and decreased in the same manner as wild type in stage 17A and B (Fig. 3K and L). The key observation was that PIN3 abundance in the replum and valve margin was similar in the *ind* mutant (Fig. 3F-H), whereas it was reduced in the valve margin compared to the replum in wild type fruit (Fig. 3B-D and M).

These data show that in valve margins of wild-type stage 14 fruit, an increase in auxin response coincides with an increase in PIN3-GFP abundance, whereas no increase in auxin response is observed in the *ind-2* mutant, most likely because of the relatively higher PIN3 plasma membrane abundance in the valve margin of this mutant at stage 14.

PID overexpression leads to patterning defects, but not indehiscence

According to previous data and models, IND represses *PID* expression whilst promoting *WAG2* expression, resulting in lateralization of PIN3 thereby generating an auxin minimum in the valve margins of stage 17B fruit (Girin et al., 2011; Sorefan et al., 2009). In line with these data and models, no PID-YFP signal could be detected in the valve margins of developing gynoecia or fruits (Fig. S4A), whereas the *WAG2* promoter was shown to be specifically active in valve margins of developing gynoecia (Girin et al., 2011).

This implies that *PID* overexpression or *wag2* loss-of-function should result in indehiscent fruits. PID and WAG2 are part of the AGC3 subclade of plant AGCVIII protein serine/threonine kinases in *Arabidopsis*, which includes two other kinase WAG1 and AGC3-4 (Galván-Ampudia and Offringa, 2007). Previously, it was shown that PID, WAG1 and WAG2 are functionally redundant (Cheng et al., 2008; Dhonukshe et al., 2010). Strong *pid* alleles are unable to produce fruits, thus we investigated dehiscence zone formation in *wag2* single and *wag1 wag2* double loss-of-function mutants. Close examination of the mature fruit of both mutants showed that dehiscence zone formation was not affected (Fig. 4F-I)

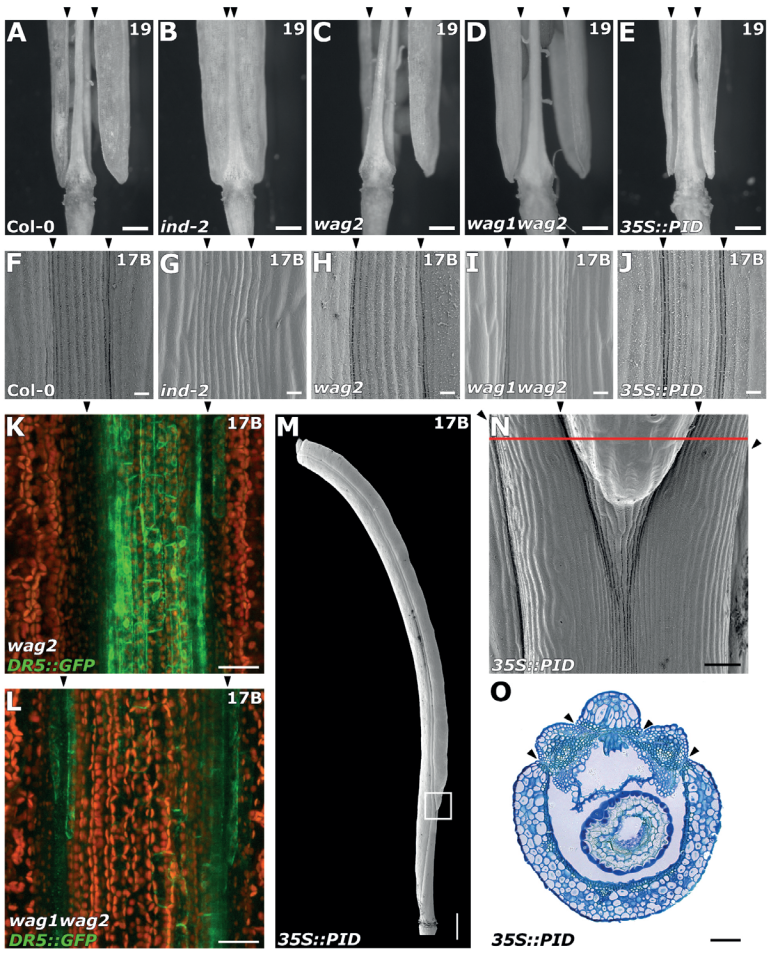

Figure 4: *wag1 wag2* loss-of-function or *35S::PID* do not affect dehiscence zone formation.
(A-E) Images of the lower part of completely dried wild-type (A), *ind-2* (B), *wag2* (C), *wag1wag2* (D), *35S::PID* (E) fruit at the moment of valve separation. (F-J) Scanning electron micrographs of the valve margins (black arrow heads) of wild-type (F), *ind-2* (G), *wag2* (H), *wag1wag2* (I) and *35S::PID* (J) fruit. (K-L) Tangential confocal images through the epidermis of stage 17B *DR5::*GFP *wag2* or *DR5::*GFP *wag1 wag2* fruit, showing an auxin response minimum in the separation layer (black arrow heads). (M-O) Valve patterning defects in stage 17B *35S::PID* fruits as observed by scanning electron microscopy ((N) shows a detailed view of the boxed area in (M)), or in a transverse toluidine blue stained section (O) at the height of unequal valve separation, as indicated by the red line in (N). Black arrowheads indicate the positions of the valve margins. Scale bar indicates 100 µm in (A-E), 10 µm in (F-J), 25 µm in (K-L), and 50 µm in (M-O).

and that fruits were able to open normally upon dehiscence (Fig. 4A-C), whereas *ind-2* mutant fruits did not (Fig. 4B and G). The local auxin minimum observed in the separation layer of mature wild-type fruits was also detected in both mutant backgrounds providing further evidence that dehiscence zone formation is undisturbed in these mutants (Fig. 4K and L). Examination of fruits developing on *35S::PID* plants revealed severe defects

in valve patterning in some fruits (Fig. 4M-O). Valves initiated asymmetrically along the replum, resulting in fused repla at the base (Fig. 4N). However, normal valve patterning was restored in the more apical parts of the fruit. Although tissue patterning was partially disturbed, SEM imaging and transverse sections showed that dehiscence zone formation occurred (Fig. 4J and O) and fruits indeed opened normally upon dehiscence (Fig. 4E). These results show that simply upregulating or knocking down the expression of *PID* or *WAG2* is not sufficient to disrupt the patterning of the valve margin region.

Valve margin specific expression of *PID* and *WAG2* results in indehiscence.

Our analysis of *PID* expression in *pid PID:PID-YFP* fruits (Fig. S4A) suggested that *PID* is specifically repressed in the valve margin as early as stage 13, and according to the model (Girin et al., 2011) *WAG2* is upregulated during valve margin specification. *IND* promoter-driven *GUS* expression is valve margin specific and strong during gynoecium development (stages 11 and 12), while it is expressed in the same tissues but weaker during fruit development (stages 14-17) (Sorefan et al., 2009). This predicted that valve margin-specific expression of *PID* or *WAG2* under the *IND* promoter would respectively repress or promote dehiscence zone specification. However, introduction of either *IND::WAG2* or *IND::PID* in the *ind-2* mutant background could not rescue the *ind* phenotype. Transverse fruit sections did not show dehiscence zone cell specification, and upon fruit maturation no valve separation was observed (Fig. 5F and G). Unexpectedly, introduction of either *IND::PID* or *IND::WAG2* expression in wild-type background resulted in indehiscent fruit in 20% (n=21) and 30% (n=26) of the transformants, respectively. Semi quantitative RT-PCR on RNA isolated from stage 13 to 17 indehiscent fruits confirmed that *IND* itself was not silenced (Fig. S5A) and that in the *IND::PID* transgenic lines *PID* was ectopically expressed (Fig. S5B). It has to be noted here that the *IND* transcript could still be detected in the *ind-2* mutant, since this allele has a frameshift mutation that causes an early stop in translation, which does not affect transcription (Liljegren et al., 2004). Transverse sections of the *IND::PID* and *IND::WAG2* transformants showed that they mimicked the *ind-2* phenotype, and that they lacked the sutures between the replum and valves that are characteristic for the valve margin and dehiscence zone (Fig. 5A-D). Valve margin specific expression of *WAG1* or *AGC3-4* did not result in indehiscent fruit in 24 T1 plants (Fig. 5E) indicating that the indehiscent phenotype is specific for the PID and WAG2 kinases, and corroborating that the phenotype is not merely caused by silencing of the *IND* gene through the introduction of one or more extra copies of the *IND* promoter. Our results on the valve margin-specific expression of *PID* and *WAG2* suggest that both *PID* and *WAG2* expression needs to be repressed by IND during dehiscence zone specification.

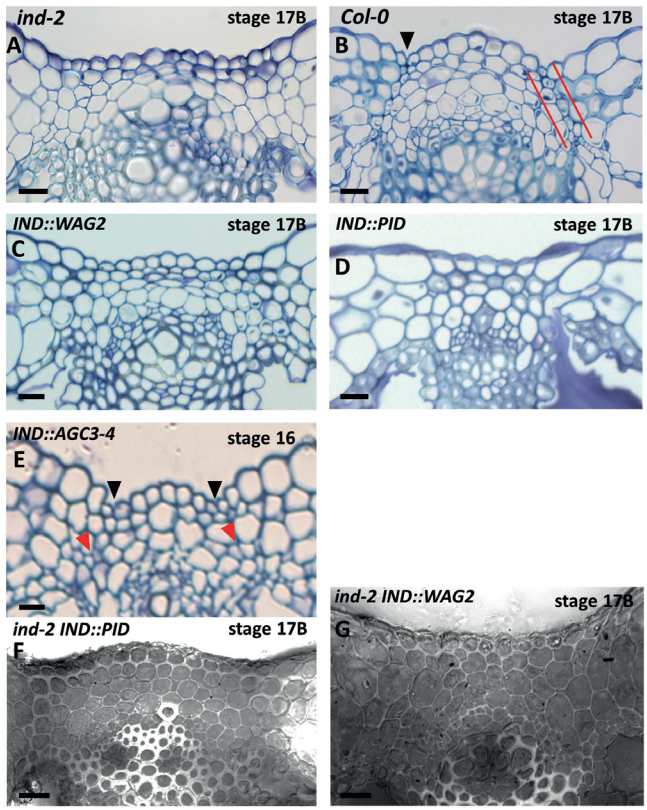

Figure 5: *IND::PID* and *IND::WAG2* mimic *ind* loss-of-function.
(A-G) Images of median transversal sections of *ind-2* (A), wild type (B), *IND::WAG2* (C), *IND::PID* (D), *IND::AGC3-4* (E), *ind-2 IND::PID* (F), *ind-2 IND::WAG2* (G). (A-E) stained with toluidine blue, while (F,G) are not.

4

Valve margin specific expression of PID and WAG2 leads to an increase in PIN3-GFP in the valve margin.

Our previous observations suggested that IND repression of *PID* (and according to our data also of *WAG2*) in the valve margins of 14-16 stage fruit is required to reduce PIN3-GFP abundance, allowing an increase in auxin response that is crucial during these stages for dehiscence zone specification. PIN3-GFP levels were indeed significantly higher in the valve margins of stage 16 *ind-2* mutant fruit, where it showed a more predominant rootward/shootward polar localization, compared to wild-type fruit (Fig. 3F-H; Fig. 6A and B). *IND::PID* and *IND::WAG2* fruit showed similar enhanced PIN3-GFP levels in the valve margins (Fig. 6C and D), compared to wild-type fruit (Fig. 6A), and these enhanced levels correlated with a reduced expression of the *DR5::GFP* auxin response reporter (Fig. 6E-G). Our results are in line with a model that dehiscence zone specification occurs at stage 14-16 of fruit development, and that at these stages an elevated auxin response rather than an auxin minimum is required for dehiscence zone specification, which is attained by IND-mediated repression of PID and WAG2 kinase expression.

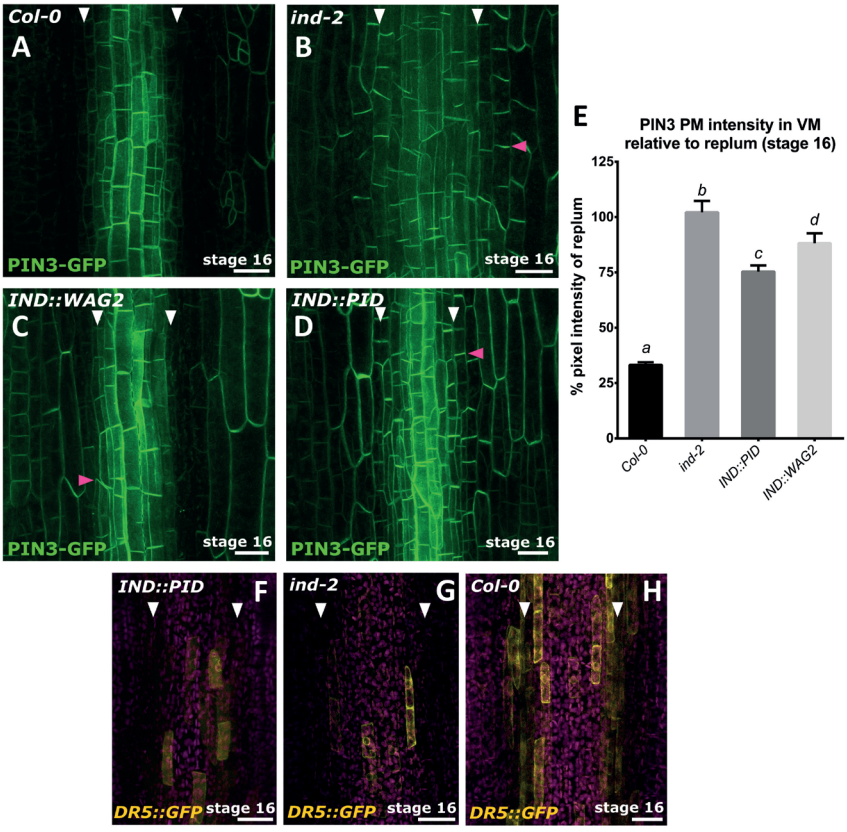

Figure 6: *IND::PID* and *IND::WAG2* show an enhancement in PIN3-GFP abundance.
Confocal microscopy images of wild type (G), *ind-2* (F), *IND::PID* (D,E) and *IND::WAG2* (C), expressing *PIN3-GFP* (green) (A-D) or *DR5::GFP* (yellow) (E-F), showing the valves, valve margin (white arrowheads) and replum at stage 16. Images were taken at the median region of the fruit. Z-stack images were projected to yield the final pictures and the magenta signal depicts the autofluorescence signal (>650nm).

Discussion

The IND transcription factor determines opening of the *Arabidopsis* fruit by specifying the dehiscence zone in the valve margin between the valve and replum (Liljegren et al., 2004). Previous research has led to the model that IND dimerizes with SPT to bind the *PID* and *WAG2* promoters, leading to repression of *PID* expression and upregulation of *WAG2*. This in turn enhances the plasma membrane abundance of PIN3, causing an auxin minimum in the dehiscence zone of stage 17B fruit, which is needed to specify the separation layer (Ding et al., 2011; Girin et al., 2011; Sorefan et al., 2009). While investigating the antagonistic function of PID and WAG2 in this developmental process, we looked more in detail into the timing of events during dehiscence zone specification. Our data show

that the cell divisions that create the separation layer in the valve margin first occur just after pollination in stage 14 fruit (for model, see Fig. 7). Interestingly, the start of these divisions coincided with an increase in auxin in the valve margin, which is different from the requirement for an auxin minimum later in fruit development to initiate separation (Sorefan et al., 2009). The auxin levels in the developing dehiscence zone increase until stage 15 and lower slightly towards stage 17A, followed by the rapid formation of an auxin minimum in the separation layer of the mature fruit. We propose that both *PID* and *WAG2* are repressed by IND, which is strongly expressed during early fruit development, and that this lowers PIN3 levels relative to the replum, resulting in a net influx of auxin into the valve margin at stages 13 and 14 (Fig. 7). The amount of auxin available increases at those stages (Sorefan *et al.,* 2009) due to the developing ovules, which are known to promote fruit growth (Dorcey et al., 2009; Fuentes et al., 2012), and we speculate that this auxin may also induce the creation of the dehiscence zone. The increase in auxin levels in turn promotes PIN3 plasma membrane abundance (Paciorek et al., 2005), causing auxin efflux and the subsequent drop in PIN3 abundance from stage 15 onwards. The true auxin minimum occurs only at the end of dehiscence zone formation (stage 17B) and may therefore mediate the final cell dissolution rather than separation layer differentiation. Our model explains why valve margin specific expression of *PID* and *WAG2* induces indehiscence. Expression of these kinases stimulates the plasma membrane abundance of PIN3, thereby preventing the moderate increase in auxin levels that induces the cell divisions leading to separation layer formation.

This model predicts that an elevated auxin response during early fruit development is necessary for separation layer specification, whereas *IND* promoter-driven expression of the bacterial auxin biosynthesis gene *iaaM* suggested that elevated auxin levels result in an indehiscent phenotype (Sorefan et al., 2009). Most likely the timing and the level of the auxin response are important here. In stage 13 fruit, auxin responses are low and in stages 14 to 16 only a moderately elevated auxin response was observed in the valve margin (Fig. 2 and 3). Most likely, the auxin levels and responses induced by *IND::iaaM* expression are too high for these early stages of fruit development, and act inhibitory on the cell division and -differentiation processes that are required to specify the dehiscence zone.

Our model differs from the earlier reported model where IND and SPT upregulate *WAG2* expression and repress *PID* expression (Girin et al., 2011; Sorefan et al., 2009). The indehiscence caused by ectopic valve margin-specific expression of *WAG2* suggests that its downregulation rather than its upregulation is necessary for separation layer specification. In our new model, IND and SPT have a common repressive effect on both genes, which seems to be a more simple scenario that is in line with the earlier reported redundant action of *PID* and *WAG2* (Dhonukshe et al., 2010). The previously reported differential regulation of *PID* and *WAG2* is based on qRT-PCR analysis on RNA extracted from 7 day old DEX-induced *35S::IND-GR* seedlings or from whole wild-type, *ind*-2 and

ful (*IND* overexpression) mutant stage 15 fruit (Sorefan et al., 2009). However, based on the analysis of *PID::PID-VENUS* (Fig. S4) and *pWAG2-GUS* (Girin *et al*., 2011) reporter lines both genes are not expressed in the valve margins after anthesis. For *WAG2* this result is surprising, since IND is expressed in developing fruit up to stage 17, and thus one would expect the *WAG2* promoter to be active during these stages. This suggests that *WAG2*, although activated by ectopically expressed IND, does not play a role in dehiscence zone specification. More cell-type specific methods, such as laser microdissection, could be used to verify the effects of IND and SPT on *PID* and *WAG2* expression in the dehiscence zone at RNA level. Our results suggest that repression of the expression of both kinase genes is essential to reduce PIN3-GFP abundance for separation layer specification. Although we cannot exclude, that *IND* promoter-driven misexpression of *PID* and *WAG2*, like for the *iaaM* gene, has yet unforeseen effects on auxin dynamics during crucial developmental stages, our results are in line with a redundant rather than a differential developmental role for these kinases.

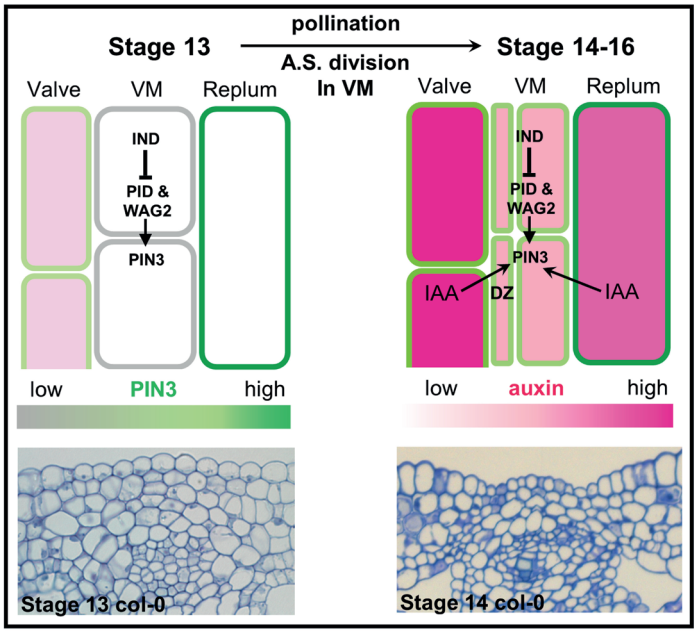

Figure 7: IND specifies the dehiscence zone in stage 14-16 fruit by repressing *PID* and *WAG2* expression. Model depicting the transition towards dehiscence zone (DZ) specification. Auxin levels are depicted in a pink fill, while PIN3-GFP plasma membrane levels are depicted in a green outline.
At stage 13 pollination takes place and fertilization at stage 14. The developing ovules cause an influx of auxin trough the replum, while the biosynthesis of auxin in the valves increases as well. PIN3 at stage 13 is present in the replum and somewhat in the valves. IND represses *PID* and *WAG2*, thereby decreasing PIN3 plasma membrane abundance. At stage 14 the increase in auxin in valves and replum causes an auxin influx into the valve margin, which has a net auxin influx due to the relatively low PIN3 plasma membrane abundance. Auxin itself promotes PIN3 at the plasma membrane through inhibition of endocytosis (Paciorek et al., 2005), creating subsequent auxin efflux. This results in a medium amount of auxin, which is beneficial for the asymmetric (A.S.) divisions specifying the dehiscence zone (DZ).

Differential plasma membrane abundance of PIN3-GFP and the resulting auxin levels are known to be instrumental in modulating cell divisions during stomatal development. Here auxin depletion, coinciding with reduced PIN3-GFP expression, triggers a developmental switch allowing the symmetric division of the guard mother cell that generates the two guard cells (Le et al., 2014). An auxin minimum and reduced PIN3-GFP abundance were also observed in the dehiscence zone in stage 17B fruit, but here there is no evidence that the minimum triggers symmetric cell divisions. The auxin minimum at stage 17B may thus be of an instructive nature and act as a final cue in specifying the cell fate of the separation layer (Fig. 7). This process could be regulated by ALC (Rajani and Sundaresan, 2001), since *alc* fruits develop a dehiscence zone with characteristic sutures, but remain indehiscent.

In contrast to the final symmetric cell division that forms the stoma, the cell divisions that generate the dehiscence zone in stage 14-16 fruit seem asymmetric, as transverse sections through developing fruit suggest that smaller cells are formed from the larger cells in the developing valve margin (Fig. 1). Due to the tapered nature of these separation layer cells it is difficult to determine their exact shape and size, and 3D-time lapse imaging would be needed to resolve this issue. Still, asymmetry of the cell divisions generating the separation layer would be more in line with their formative nature, and with our observations that a mild elevation in auxin response, rather than auxin depletion, occurs in the valve margin of stage 14-16 fruit.

In conclusion, we propose that IND facilitates this early specification of the dehiscence zone, which is missing in *ind-2* fruit, by repressing PID and WAG2, thereby precisely controlling the auxin levels in the dehiscence zone through PIN3-mediated auxin efflux and instructing formation of the separation layer.

Materials and Methods

Plant lines and plant growth

All *Arabidopsis* lines are in the Col-0 background. The *wag1* (SALK_002056), *wag2* (SALK_070240) mutant alleles (Santner and Watson, 2006), and the transgenic lines *35S::PID-venusYFP* (Michniewicz et al., 2007), *35S::DII-venusYFP* and *35S::mDII-venusYFP* (Brunoud et al., 2012), *ind-2 DR5::GFP* and *ind-2 PIN3-GFP* (Sorefan et al., 2009) have been previously described. *wag2 DR5::GFP* and *wag1wag2 DR5::GFP* plants were selected from earlier described *wag2 pid14+/- DR5::GFP* and *wag1wag2 pid14+/- DR5::GFP* lines (Dhonukshe et al., 2010). The *pin3 PIN3::PIN3-GFP DR5::RFP* line was obtained by crossing the previously described *pin3 PIN3::PIN3-GFP* line (Friml et al., 2002) with the *DR5::RFP* line (Marhavý et al., 2011). Primers for genotyping are listed in Table S1 (primers 1-3). All plants were grown under long-day conditions (16/8 hrs light/dark), at 21°C and 70% RH.

Molecular cloning

The *IND* promoter was PCR amplified from the *proIND::IND-GUS* template plasmid (Sorefan et al., 2009) using primer pair 12 and 13 (Table S1). The proIND fragment was cloned into the *Asc*I digested pGreenII based gateway tagRFP containing vector, upstream of the Gateway cassette and the *tagRFP* gene. The *PID*, *WAG2, AGC3-4* and *WAG1* coding sequences (Dhonukshe et al., 2010) were Gateway-recombined into this destination vector, generating the final *proIND::PID*(or *WAG1/WAG2/AGC3-4*)-*tagRFP* constructs. All primer sequences used for the molecular cloning are listed in Table S1.

Plant transformation and selection

The constructs *proIND::PID:tagRFP* and *proIND::WAG2:tagRFP* were introduced into *Agrobacterium* strain AGL1 by electroporation and transgenic *Arabidopsis* lines were obtained by floral dip transformation (Davis et al., 2009). Primary transformants were selected using 30 ug/ml phosphinothricin (PPT (duchefa)) and single locus homozygous T2 plants were selected on 30 ug/ml PPT and transferred to soil to be assessed for separation layer defects, either by assessing fruit opening upon complete maturation of the fruit, or by investigating separation layer formation in transverse hand sections of the middle of stage 17B fruits.

RNA isolation and RT-PCR

Staged gynoecia and fruits were ground and used for an RNA extraction using a Nucleospin RNA kit (Machery-Nagel). The resulting RNA was used in a first strand synthesis reaction with M-MLV Reverse Transcriptase (according to manual: Promega) and the resulting cDNA was used as a template for a conventional PCR reaction with 29 cycles to amplify products of either *IND* (primers 10 and 11), *tagRFP* (primers 8 and 9) or *UBQ10* (primers 14 and 15) (Table S1).

Microscopy and embedding

All samples for embedding and scanning electron microscopy (SEM) were fixed overnight in 2% paraformaldehyde and 1% glutaraldehyde in 1X Phosphate Buffered Saline (PBS, pH7). Fixed samples were subsequently dehydrated in an increasing range of alcohol (for embedding) or acetone (for SEM). For embedding, the middle 5 mm of the fruit was incubated in propylene oxide for 2x 15 min. at room temperature (RT), then transferred to a 1:1 mixture of propylene oxide and Epon for 2 hrs at RT. Fresh Epon was added and samples were incubated overnight and placed in silicon moulds the following day. Polymerisation of the Epon was conducted at 60°C for 2 days. Histological sections were prepared using a Leica RM 2165 rotary microtome, in combination with handmade glass

knives. Sections were made in the range of 2-3 µm and placed in water, then heat-fixed to the object glass using a hot plate. Sections were stained with 0.1% toluidine blue solution for 1 minute, rinsed with demineralised water and dried at 37°C for 2 days. Sections were mounted in Epon and polymerisation was done at 60°C overnight. Images were obtained using the Zeiss Axioplan 2 microscope, equipped with a Zeiss AxioCam MRc 5 digital colour camera.

After acetone dehydration, SEM samples were dried using the Bal-Tec CDP030 critical point dryer and samples were fixed to stubs to be coated with gold using the SEM Coating unit 5100 (Polaron Equipment Ltd.). Samples were viewed using the JEOL SEM 6400 scanning electron microscope.

Confocal microscopy was performed using either an inverted Zeiss LSM5 Exciter / AxioObserver or an upright Zeiss LSM5 Exciter / AxioImager confocal laser scanning microscope. Whole-mount fruits were viewed immediately after collection, using a 40x long working distance water immersion objective. Lasers and bandpass filters used: GFP, 488 nm laser, 505-530 nm filter; YFP, 514 nm laser, 530-560 nm filter; RFP, 543 nm laser; autofluorescence was captured with a 650 nm long pass filter. To reduce water tension, samples were first washed in a 1% Tween solution, rinsed thoroughly with demineralised water, and fixed to object glasses using superglue. Autofluorescence was detected using a 650 nm long-pass filter. All images were processed using either ImageJ, ICY (http://icy.bioimageanalysis.org/), GIMP (http://www.gimp.org) or Adobe Photoshop CS5 (http://www.adobe.com).

Acknowledgements

We would like to thank Lars Østergaard for providing various reporter lines in wild-type and *ind-2* mutant background and the *IND* promoter clones; Eva Benkova for providing the *DR5::RFP* line. Moreover, we are grateful to Lars Østergaard and to Emma Larsson for critical comments on the manuscript.

References

Benjamins, R., Quint, A., Weijers, D., Hooykaas, P. and Offringa, R. (2001). The PINOID protein kinase regulates organ development in *Arabidopsis* by enhancing polar auxin transport. *Development* **128**, 4057–67.

Benková, E., Michniewicz, M., Sauer, M., Teichmann, T., Seifertová, D., Jürgens, G. and Friml, J. (2003). Local, efflux-dependent auxin gradients as a common module for plant organ formation. *Cell* **115**, 591–602.

Boer, D. R., Freire-Rios, A., van den Berg, W. a M., Saaki, T., Manfield, I. W., Kepinski, S., López-Vidrieo, I., Franco-Zorrilla, J. M., de Vries, S. C., Solano, R., et al. (2014). Structural Basis for DNA Binding Specificity by the Auxin-Dependent ARF Transcription Factors. *Cell* **156**, 577–89.

Brunoud, G., Wells, D. M., Oliva, M., Larrieu, A., Mirabet, V., Burrow, A. H., Beeckman, T., Kepinski, S., Traas, J., Bennett, M. J., et al. (2012). A novel sensor to map auxin response and distribution at high spatio-temporal resolution. *Nature* **482**, 103–106.

Cheng, Y., Qin, G., Dai, X. and Zhao, Y. (2008). NPY genes and AGC kinases define two key steps in auxin-mediated organogenesis in *Arabidopsis*. *Proc. Natl. Acad. Sci. U. S. A.* **105**, 21017–22.

Davis, A. M., Hall, A., Millar, A. J., Darrah, C. and Davis, S. J. (2009). Protocol: Streamlined sub-protocols for floral-dip transformation and selection of transformants in *Arabidopsis thaliana*. *Plant Methods* **5**, 3.

De Smet, I. and Beeckman, T. (2011). Asymmetric cell division in land plants and algae: the driving force for differentiation. *Nat. Rev. Mol. Cell Biol.* **12**, 177–88.

Dhonukshe, P., Huang, F., Galvan-Ampudia, C. S., Mähönen, A. P., Kleine-Vehn, J., Xu, J., Quint, A., Prasad, K., Friml, J., Scheres, B., et al. (2010). Plasma membrane-bound AGC3 kinases phosphorylate PIN auxin carriers at TPRXS(N/S) motifs to direct apical PIN recycling. *Development* **137**, 3245–55.

Ding, Z., Galván-Ampudia, C. S., Demarsy, E., Langowski, L., Kleine-Vehn, J., Fan, Y., Morita, M. T., Tasaka, M., Fankhauser, C., Offringa, R., et al. (2011). Light-mediated polarization of the PIN3 auxin transporter for the phototropic response in *Arabidopsis*. *Nat. Cell Biol.* **13**, 447–52.

Dorcey, E., Urbez, C., Blázquez, M. A., Carbonell, J. and Perez-Amador, M. A. (2009). Fertilization-dependent auxin response in ovules triggers fruit development through the modulation of gibberellin metabolism in *Arabidopsis*. *Plant J.* **58**, 318–332.

Ferrándiz, C. (2002). Regulation of fruit dehiscence in *Arabidopsis*. *J. Exp. Bot.* **53**, 2031–2038.

Ferrándiz, C., Pelaz, S. and Yanofsky, M. F. (1999). Control of Carpel and Fruit Development in *Arabidopsis*. *Annu. Rev. Biochem.* **68**, 321–354.

Ferrándiz, C., Liljegren, S. J. and Yanofsky, M. F. (2000). Negative regulation of the SHATTERPROOF genes by FRUITFULL during *Arabidopsis* fruit development. *Science* **289**, 436–438.

Friml, J., Wiśniewska, J., Benková, E., Mendgen, K. and Palme, K. (2002). Lateral relocation of auxin efflux regulator PIN3 mediates tropism in *Arabidopsis*. *Nature* **415**, 806–9.

Friml, J., Yang, X., Michniewicz, M., Weijers, D., Quint, A., Tietz, O., Benjamins, R., Ouwerkerk, P. B. F., Ljung, K., Sandberg, G., et al. (2004). A PINOID-dependent binary switch in apical-basal PIN polar targeting directs auxin efflux. *Science* **306**, 862–5.

Fuentes, S., Ljung, K., Sorefan, K., Alvey, E., Harberd, N. P. and Østergaard, L. (2012). Fruit growth in *Arabidopsis* occurs via DELLA-dependent and DELLA-independent gibberellin responses. *Plant Cell* **24**, 3982–96.

Galván-Ampudia, C. S. and Offringa, R. (2007). Plant evolution: AGC kinases tell the auxin tale. *Trends Plant Sci.* **12**, 541–7.

Girin, T., Paicu, T., Stephenson, P., Fuentes, S., Körner, E., O'Brien, M., Sorefan, K., Wood, T. a, Balanzá, V., Ferrándiz, C., et al. (2011). INDEHISCENT and SPATULA Interact to Specify Carpel and Valve Margin Tissue and Thus Promote Seed Dispersal in *Arabidopsis*. *Plant Cell* **23**, 1–14.

Le, J., Liu, X.-G., Yang, K.-Z., Chen, X.-L., Zou, J.-J., Wang, H.-Z., Wang, M., Vanneste, S., Morita, M., Tasaka, M., et al. (2014). Auxin transport and activity regulate stomatal patterning and development. *Nat. Commun.* **5**, 3090.

Liao, C., Smet, W., Brunoud, G., Yoshida, S., Vernoux, T. and Weijers, D. (2015). Reporters for sensitive and quantitative measurement of auxin response. *Nat. Methods* 1–6.

Liljegren, S. J., Roeder, A. H. K., Kempin, S. a, Gremski, K., Østergaard, L., Guimil, S., Reyes, D. K. and Yanofsky, M. F. (2004). Control of fruit patterning in *Arabidopsis* by INDEHISCENT. *Cell* **116**, 843–53.

Marhavý, P., Bielach, A., Abas, L., Abuzeineh, A., Duclercq, J., Tanaka, H., Pařezová, M., Petrášek, J., Friml, J., Kleine-Vehn, J., et al. (2011). Cytokinin modulates endocytic trafficking of PIN1 auxin efflux carrier to control plant organogenesis. *Dev. Cell* **21**, 796–804.

Michniewicz, M., Zago, M. K., Abas, L., Weijers, D., Schweighofer, A., Meskiene, I., Heisler, M. G., Ohno, C., Zhang, J., Huang, F., et al. (2007). Antagonistic regulation of PIN phosphorylation by PP2A and PINOID directs auxin flux. *Cell* **130**, 1044–56.

Østergaard, L. (2009). Don't "leaf" now. The making of a fruit. *Curr. Opin. Plant Biol.* **12**, 36–41.

Paciorek, T., Zazímalová, E., Ruthardt, N., Petrásek, J., Stierhof, Y.-D., Kleine-Vehn, J., Morris, D. a, Emans, N., Jürgens, G., Geldner, N., et al. (2005). Auxin inhibits endocytosis and promotes its own efflux from cells. *Nature* **435**, 1251–6.

Rajani, S. and Sundaresan, V. (2001). The *Arabidopsis* myc/bHLH gene alcatraz enables cell separation in fruit dehiscence. *Curr. Biol.* **11**, 1914–1922.

Roeder, A. H. K., Ferrándiz, C. and Yanofsky, M. F. (2003). The role of the REPLUMLESS homeodomain protein in patterning the *Arabidopsis* fruit. *Curr. Biol.* **13**, 1630–1635.

Santner, A. a and Watson, J. C. (2006). The WAG1 and WAG2 protein kinases negatively regulate root waving in *Arabidopsis*. *Plant J.* **45**, 752–64.

Smyth, D. R., Bowman, J. L. and Meyerowitz, E. M. (1990). Early flower development in *Arabidopsis*. *Plant Cell* **2**, 755–767.

Sorefan, K., Girin, T., Liljegren, S. J., Ljung, K., Robles, P., Galván-Ampudia, C. S., Offringa, R., Friml, J., Yanofsky, M. F. and Østergaard, L. (2009). A regulated auxin minimum is required for seed dispersal in *Arabidopsis*. *Nature* **459**, 583–6.

Wu, H., Mori, A., Jiang, X., Wang, Y. and Yang, M. (2006). The INDEHISCENT protein regulates unequal cell divisions in *Arabidopsis* fruit. *Planta* **224**, 971–979.

Yoshida, S., Barbier de Reuille, P., Lane, B., Bassel, G. W., Prusinkiewicz, P., Smith, R. S. and Weijers, D. (2014). Genetic control of plant development by overriding a geometric division rule. *Dev. Cell* **29**, 75–87.

Supplemental data

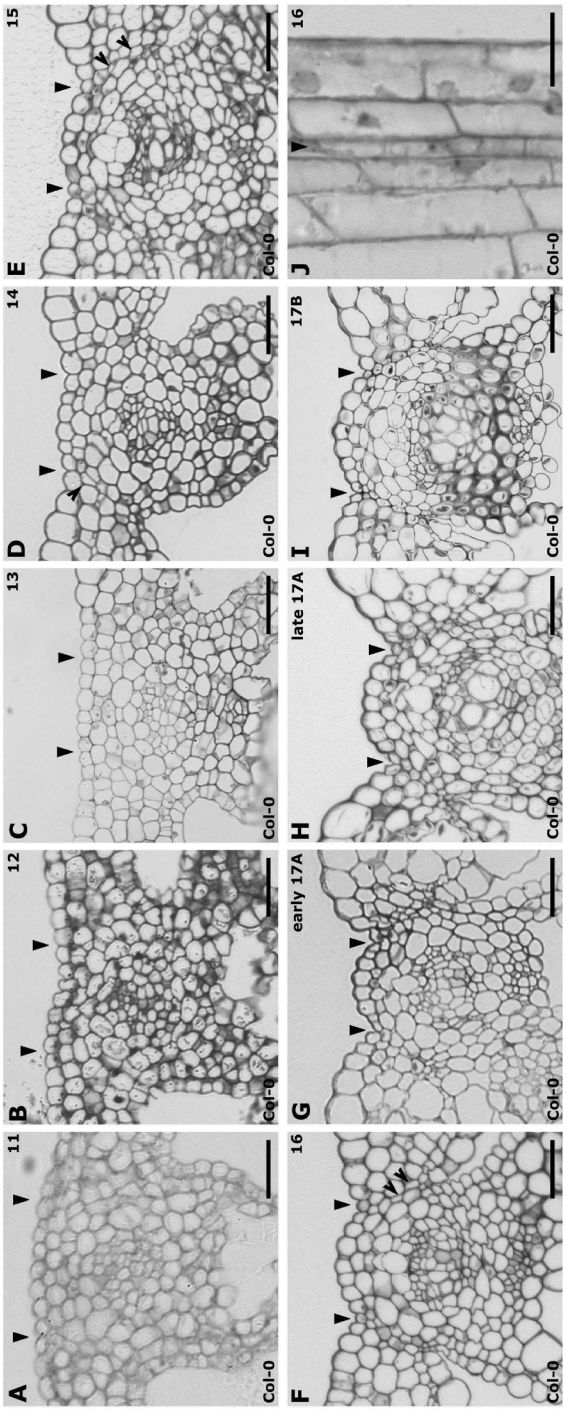

Figure S1: Dehiscence zone development in wild-type fruit.
(A-J) Median sections of wild type fruit similar to figure 1, showing stages 11-17B. In stages 14 through 16 (D-F) smaller cells appear in the valve margin (open arrowheads). These divisions might appear asymmetric depending on the positioning of the section, due to the tapered ends of the valve margin cells, shown in a transverse section (J). Scale bar = 20 µm.

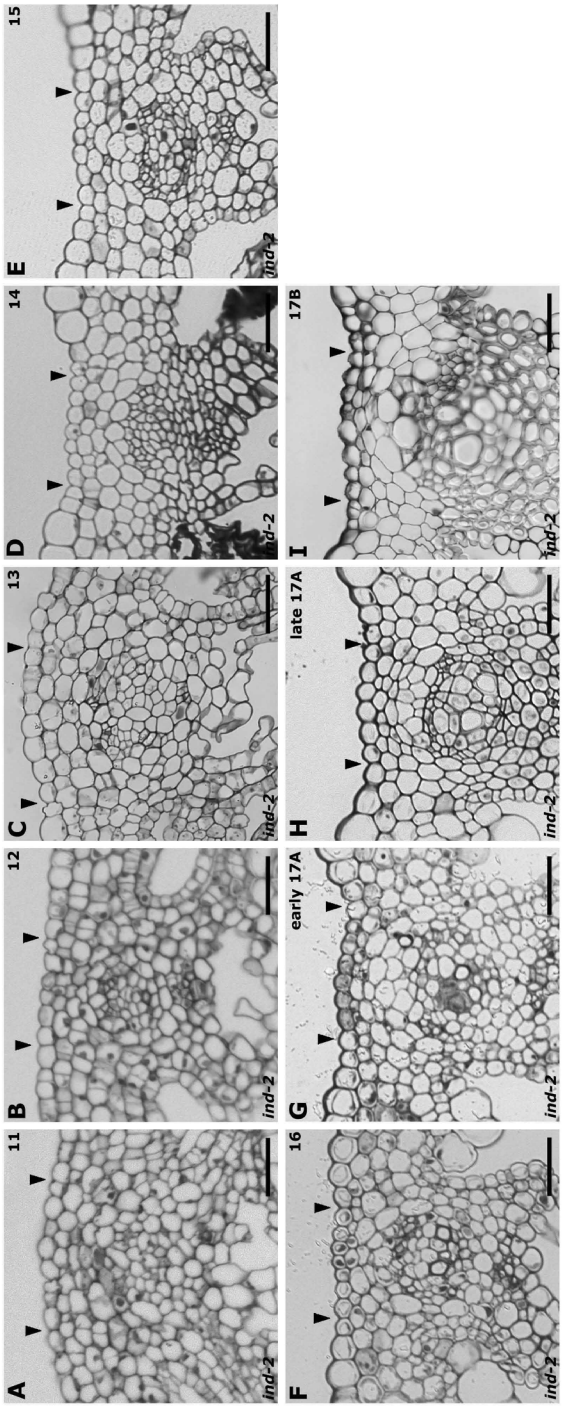

Figure S2: Absence of dehiscence zone development in the *ind*-2 mutant.
(A-I) Median sections of the *ind*-2 mutant showing stages 11 through 17B, similar as in figure 1 and S1. The absence of cell divisions and development in the valve margin (black arrows) was clear. Scale bar = 20 µm.

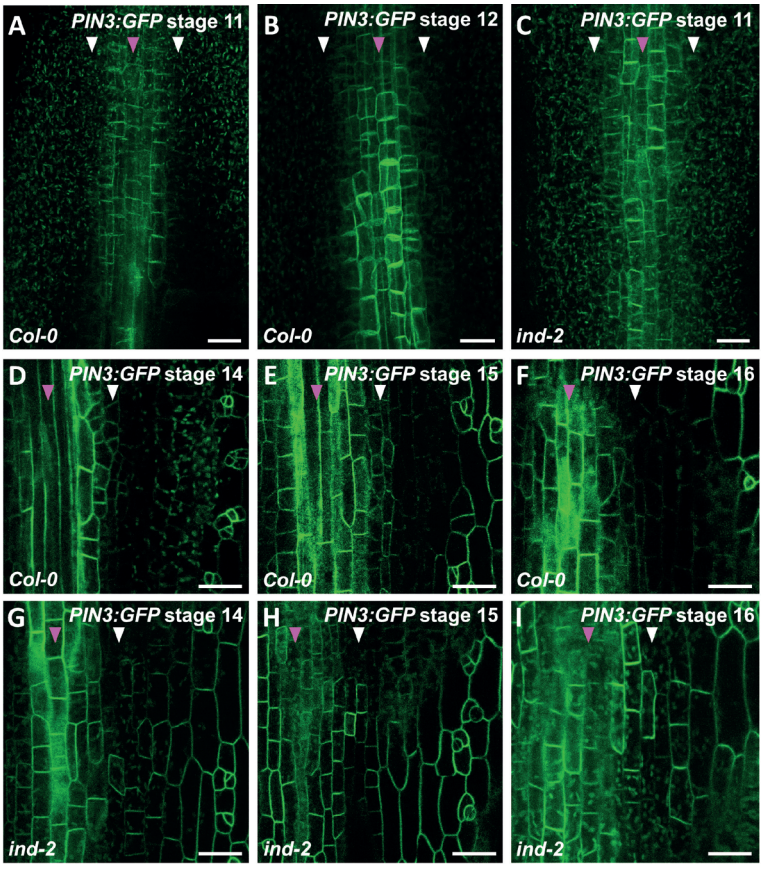

Figure S3: PIN3-GFP plasma membrane abundance is repressed in the valve margin of wild-type fruit. Confocal microscopy images of *PIN3:GFP* in wild type *Col-0* and *ind-2* fruits. White arrows show the location of the valve margin and pink arrows point towards the centreline of the replum. (A,B, D-F) PIN3-GFP was only visible in the replum at stage 11 and 12, increased at stage 14 in the valve margin and decreased at stage 16. (C, G-I) At stage 11 in *ind-2,* PIN3-GFP showed similar to wild type at this stage of fruit development, at stage 14 through 16 PIN3-GFP was strong in *ind-2* throughout the whole fruit. Scale bar = 20 µm.

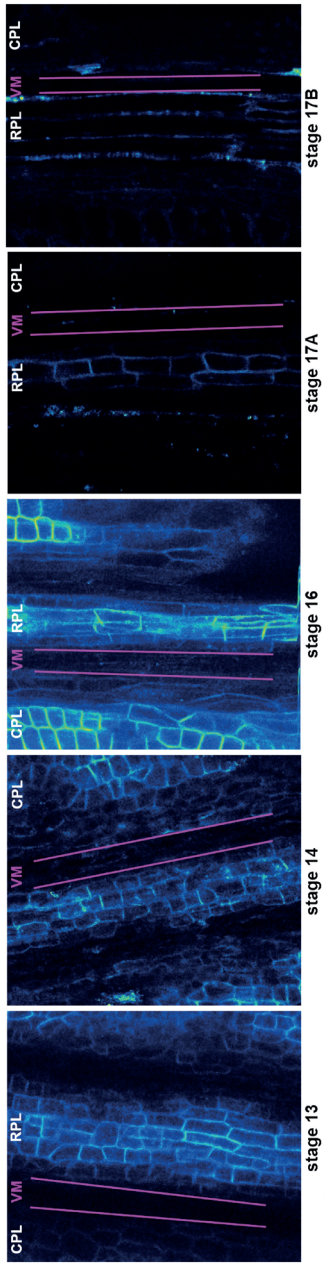

Figure S4: PID is repressed in the valve margin.
Z-stack projection of confocal images from fruits of *pid PID::PID-YFP*. The valve margin (VM) is highlighted between pink lines and flanked by the carpel (CPL) and replum (RPL). In stage 13-16 PID-YFP signal was not visible in the valve margin, while it was clearly visible on the plasma membrane in the carpel and replum. From stage 17A on, PID signal diminished, which coincides with diminished PIN3-GFP at this developmental stage (Fig. 3I and J)

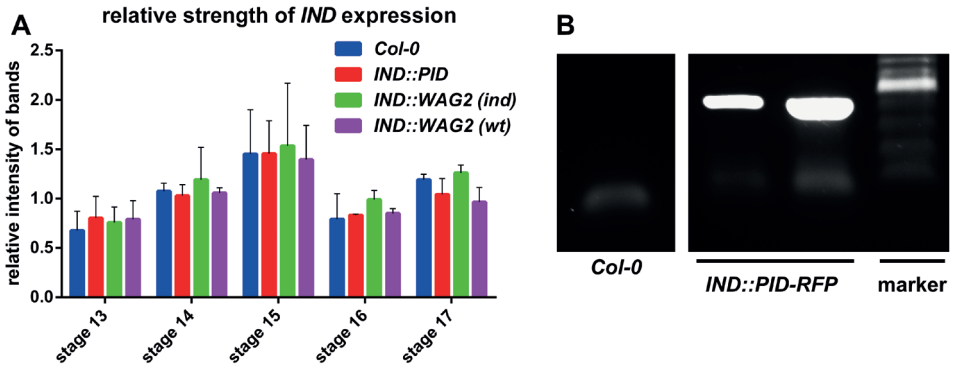

Figure S5: *IND* is not silenced in transgenic *IND::PID* and *IND::WAG2* lines.
(A) Semi quantitative RT-PCR on whole fruits of *Col-0, IND::PID* and *IND::WAG2* lines (T3 generation). Primers on the coding region of *IND* (primers 10 and 11) were used to detect expression in a semi-quantitative manner against bands produced with primers on the *UBQ10* gene (primers 14 and 15) and bands were quantified using ImageJ. (B) RT-PCR analysis onstage 15 and 16 *IND::PID:tagRFP* fruits detects *RFP* expression (transgenics are T3 generation or later) (primers 8 and 9). Lane 1 and 2 show *RFP* transcript, while lane three contains the Fermentas 1kb plus size marker.

Table S1. Primers used for genotyping and molecular cloning and expression analysis.

	Name	Sequence
1	pid-14 LP	CAGTCGGGAAACTCAACTGTC
2	pid-14 RP	ATTTTGCGATGAAAGTTGTGG
3	LBb1.3	ATTTTGCCGATTTCGGAAC
4	PIDcds F	GATTTACACTCTCTCCGTCA
5	WAG2cds F	CTTTTAAATCTCGTCGCTACC
6	M13_F	CGCCAGGGTTTTCCCAGTCACGAC
7	M13_R	TCACACAGGAAACAGCTATGAC
8	tagRFP 422bp FW	AACCTTCATCAACCACACCC
9	tagRFP 422bp rev	CTCTTTGTCGGCCTCCTT
10	IND RTPCR 02 FW	CAAACACCACACGTCCACT
11	IND RTPCR 02 R	AGGCCCGAAACCACATCA
12	proIND AscI F	aaaaggcgcgccCCTTATGTTAATATCACCGTAGGC
13	proIND AscI R	ttttggcgcgccGCTTCTTTTGGGGCTGTGGTTGGA
14	UBQ10-388-F	AGAACTCTTGCTGACTACAATATCCAG[1]
15	UBQ10-494-R	ATAGTTTTCCCAGTCAACGTCTTAAC[1]
16	AGC3-4 cds F	TCATCTCCTGCTTCTCTCC
17	WAG1 cds F	TTCTCACTATACTTGCCTCCT

[1]Girin *et al.*, 2011